Vortices and strings in a model ecosystem

Kei-ichi Tainaka
Department of Physics, Ibaraki University, Mito, Ibaraki 310, Japan
(Received 4 April 1994)

We study the spatial pattern formation in a model ecosystem by the position-fixed reaction method. This ecosystem contains three biospecies whose competing powers are cyclic. It is well known that this system is self-organized into a *quasistationary* state, and that the mean-field approximation (MFA) never predicts such a pattern formation. Recently, several authors applied the pair approximation (PA), and obtained considerable improvements. However, applying PA to our ecosystem fails to yield such an improvement as revealed by computer simulations. The failures of MFA and PA may be attributed to the fact that both approximations neglect a long-range correlation. Thus we introduce the concept of topological defects, such as "vortices" or "strings," and demonstrate that the dynamics of these defects can at least qualitatively account for the observed pattern formation dynamics.

PACS number(s): 02.50.−r, 87.10.+e, 64.60.Cn, 82.20.Wt

I. INTRODUCTION

Spatial patterns in various complex systems are intensively investigated by many authors [1]. In general, it is very difficult to give a theoretical account on the dynamics of the spatial pattern formed. This difficulty mainly comes from the fact that the degree of freedom of space is infinite. In this article, we introduce the concept of topological defects [2] to understand the pattern dynamics. Since the number of topological defects is not so great, the pattern formation process of the system is much simplified. The importance of such a mesoscopic (coarse-grained) picture is widely recognized in many areas [3].

In most cases, large interactive systems organize themselves into stationary states. Note that "stationary" is not synonymous with "equilibrium." When the principle of detailed balance is broken, the stationary state is in fact in nonequilibrium. Such a state is said to be in "cyclic balance" [4]. A typical example of nonequilibrium systems is an ecosystem where the cyclic balance is maintained by a food chain (web). In the present paper, we examine a basic cyclic system whose reaction rule is the same as that of the so-called "paper, scissors, stone" (PSS) game [5–7]. The PSS system is one of the simplest ecological models and is defined in Sec. II.

Until recently, the pattern formation for model ecosystems has been investigated by the use of diffusion-reaction equations [8], which are represented by the sum of the reaction and diffusion terms. In most cases, the former term is called the Lotka-Volterra model [9]. However, reaction-diffusion approaches have several limitations [10,11]. (i) In the reaction term, the effect of spatial correlation is neglected. (ii) It is very hard to obtain a "quasistationary state," where the average density of each species is unchanged with time but the local density of the species varies dynamically.

Recently, lattice models such as the cellular automaton [12] and the coupled map lattice [13], have received growing interest in connection with the development of computers. Although the lattice model is an oversimplification for real systems, one can get valuable information on nonlinear complex problems. In particular, the lattice model is useful to obtain the quasistationary pattern and to take into account the effect of spatial correlation. It is, however, still difficult to undertake a theoretical investigation.

In the present article, we deal with a chemical reaction on lattice spaces. In the case of the chemical reaction, the mean-field theory, which is often called the Lotka-Volterra model, is well established. From the key words "chemical reaction" and "lattice model," one may imagine the diffusion-controlled reaction [14] where each reactant can move randomly. This reaction system, however, has the following disadvantages [15]. (i) It requires long computation time to carry out simulations. (ii) It is very difficult to give theoretical approaches. These disadvantages have origins in the diffusion process of reactants.

For this reason, we apply the position-fixed reaction (PFR) [10, 16–18], which is equivalent to the contact process [19–21]. Simulations for the PFR are carried out under the assumption that each reactant (individual) on a lattice site never moves. This assumption may be applicable for plants and approximately valid even for animals, provided that the radius of action of an individual is much shorter than the size of the whole system.

One of the most interesting results of position-fixed reactions may be the "uncertainty (unpredictability) theory" for biospecies extinction [10]: one cannot predict the extinction of biological species nor pursue the cause of extinction. This unpredictability is essentially different from that in chaotic motion and practically destroys the concept of natural selection in Darwinian arguments [22]. Although to some extent the unpredictability is due to the complexity of the systems, it is largely due to the "phase transition" and "indirect effect." In general, the phase transition has the property that a major result is brought about by minor causes. On the other hand, the indirect effect means that there is no direct relation between the cause and result [23]. It is, therefore, hopeless

 ©1994 The American Physical Society

to determine the minor cause of the phase transition (extinction), since the cause is not directly related to the extinction.

So far, many physicists have intensively investigated the phase transition. On the other hand, very few know the indirect effect. The study on the spatial pattern formation reveals that this effect brings about many paradoxical results [10,11,16,17] and that outcomes due to the indirect effect are very sensitive to various factors, such as values of interaction parameters [10]. In order to understand the importance of the indirect effect, it is necessary to develop theoretical approaches.

However, at the present stage, the mathematical treatment for the position-fixed reaction (PFR) is too restricted. Even in two-state models (each lattice site takes on the value of either $+1$ or -1), exact results have not yet been obtained [24]. Heretofore, several approximation theories have been presented. Above all, the mean-field theory is very important, since it is the first order approximation for PFR. Nevertheless, this theory never gives a sufficient prediction about the result of PFR. Recently, Katori and Konno [21] applied the second order theory known as pair approximation (PA). After that work, several authors [10,11,17,25] applied the pair approximation (PA) to various position-fixed reactions and obtained more preferable results than those predicted by the mean-field approximation (MFA).

In the present article, we apply the PA to the PSS system to explain the pattern formation dynamics observed in the lattice model of the PFR. However, computer simulations reveal that the PA model never gives a comfortable result, even compared to the mean-field approximation. Both these approximations fail because they neglect the long-range correlation, whose existence is confirmed by a numerical analysis.

To explain the pattern formation in the PSS model, we introduce the concept of topological defects such as "vortices" and "strings." It is demonstrated that the dynamics of these defects can at least qualitatively account for the observed pattern formation dynamics. The pattern process of the lattice system is thus simplified by such a mesoscopic (coarse-grained) picture.

This article is a full length version of Ref. [2]. However, in this article we emphasize the following points for the first time. (i) We examine the population dynamics of the pair approximation, and demonstrate that the PA never explains the dynamics of the PFR (Sec. III). (ii) We show examples of the effect of long-range correlation (Sec. IV). Hence, it is found that the concept of topological defects is still useful to account for the pattern formation in the PSS model (Sec. V).

II. MODEL AND MASTER EQUATIONS

We consider a basic cyclic system in which many individuals (particles) of three species 1, 2, and 3 are contained. The interaction between particles is assumed to be represented by the rules of the paper, scissors, stone game,

$$X_1+X_2\rightarrow 2X_1 , \tag{1a}$$

$$X_2+X_3\rightarrow 2X_2 , \tag{1b}$$

$$X_3+X_1\rightarrow 2X_3 , \tag{1c}$$

where X_i denotes the individual (particle) of species i. In this case, three species have the cyclic strength; the species i is "stronger" than species $i+1$, where $i+3=i$. It is emphasized that the system (1) has the "cyclic symmetry," namely, our system is unchanged, even if every species i ($i=1,2,3$) is changed to $i+1$. Because of cyclic symmetry, there is no dominant species in the hierarchy.

The random collision model (mean-field limit) of the PSS game was first studied by Itoh [5]. He obtained the result that the population dynamics reveals a "neutrally stable center"; the population size of each species oscillates around the fixed point where three species coexist with equal densities. The oscillation profile depends on initial conditions.

On the other hand, the lattice model (PFR) for the rule (1) has been studied by the present author [6] and by Bramson and Griffeath [7]. The former work first demonstrated that the spatial pattern on two-dimensional lattice space naturally evolves into a quasistationary state. Such a pattern is self-organized irrespective of initial patterns. Photographs of typical patterns are illustrated in Fig. 1, where (a) and (b) represent the initial random distribution and final stationary pattern, respectively.

Let P_i be the density of species i ($\sum_i P_i=1$); then the master equations for the system (1) in the position-fixed limit are expressed by

$$\dot{P}_1=2P_{12}-2P_{31} , \tag{2a}$$

$$\dot{P}_2=2P_{23}-2P_{12} , \tag{2b}$$

$$\dot{P}_3=2P_{31}-2P_{23} . \tag{2c}$$

Here the dot represents the derivative with respect to the time t, and P_{ij} is the two-body probability density finding a species i at a site and a species j at a nearest neighbor of that site ($i,j=1,2,3$). Time t is measured in units of Monte Carlo steps (MCS) [6]. Note that P_{ij} is the joint probability, so that the relations $P_{ij}=P_{ji}$ and $\sum_j P_{ij}=P_i$ hold.

Similarly, the master equations for the two-body probability densities are given by

$$(z/4)\dot{P}_{11}=P_{12}+(z-1)[P^2_{11}-P^1_{31}] , \tag{3a}$$

$$(z/4)\dot{P}_{22}=P_{23}+(z-1)[P^3_{22}-P^2_{12}] , \tag{3b}$$

$$(z/4)\dot{P}_{33}=P_{31}+(z-1)[P^1_{33}-P^3_{23}] , \tag{3c}$$

$$(z/2)\dot{P}_{12}=-P_{12}+(z-1)[-P^2_{11}-P^1_{23}+P^3_{12}+P^2_{12}] , \tag{3d}$$

$$(z/2)\dot{P}_{23}=-P_{23}+(z-1)[-P^3_{22}-P^2_{31}+P^1_{23}+P^3_{23}] , \tag{3e}$$

$$(z/2)\dot{P}_{31}=-P_{31}+(z-1)[-P^1_{33}-P^3_{12}+P^2_{31}+P^1_{31}] , \tag{3f}$$

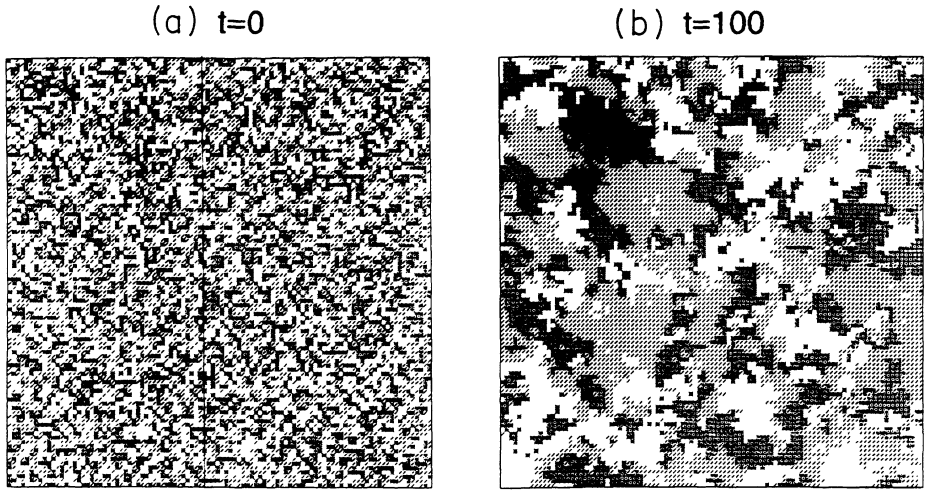

FIG. 1. Photographs of typical patterns are illustrated, where (a) and (b) represent the initial random pattern and final stationary pattern, respectively.

where P^i_{jk} denotes the three-body probability density of finding a color i at a site and colors j and k at nearest neighbors of that site, and z is the number of nearest neighbors ($z=4$ for square lattice). It is worthwhile noting that (2) are derived from (3). The master equations (2) or (3) cannot be solved, since n-body probability densities are represented by $(n+1)$-body ones.

III. NUMERICAL ANALYSIS IN THE PA LIMIT

In this section, we examine the dynamics under the pair approximation (PA), which is the second order approximation for the lattice model. This approximation is explicitly expressed by [21,10]

$$P^i_{jk}=P_{ij}P_{ik}/P_i \ . \tag{4}$$

Inserting (4) into (3), we obtain the evolution equations in the PA limit:

$$\dot{P}_{11}=P_{12}+3[(P_{12})^2/P_2-P_{31}P_{11}/P_1] \ , \tag{5a}$$

$$\dot{P}_{22}=P_{23}+3[(P_{23})^2/P_3-P_{12}P_{22}/P_2] \ , \tag{5b}$$

$$\dot{P}_{33}=P_{31}+3[(P_{31})^2/P_1-P_{23}P_{33}/P_3] \ , \tag{5c}$$

$$\dot{P}_{12}=-P_{12}+3[-(P_{12})^2/P_2-P_{31}P_{12}/P_1 +P_{31}P_{23}/P_3+P_{12}P_{22}/P_2] \ , \tag{5d}$$

$$\dot{P}_{23}=-P_{23}+3[-(P_{23})^2/P_3-P_{12}P_{23}/P_2 +P_{12}P_{31}/P_1+P_{23}P_{33}/P_3] \ , \tag{5e}$$

$$\dot{P}_{31}=-P_{31}+3[-(P_{31})^2/P_1-P_{23}P_{31}/P_3 +P_{23}P_{12}/P_2+P_{31}P_{11}/P_1] \ , \tag{5f}$$

where we assume a two-dimensional square lattice ($z=4$). The steady-state solution is easily obtained by setting all the time derivatives in (5) to be zero,

$$P_i=\tfrac{1}{3}, \quad P_{ii}=\tfrac{5}{27} \ , \quad P_{ij}=\tfrac{2}{27} \ , \tag{6}$$

where $i,j=1,2,3$ ($i\neq j$).

First, we undertake a theoretical analysis. We consider a simple case where an initial condition satisfies

$$P_{11}=P_{22}=P_{33}=P_{ii} \ , \quad P_{12}=P_{23}=P_{31}=P_{ij} \ . \tag{7}$$

In this case, the condition (7) holds at any time (cyclic symmetry). According to the mathematical relation ($\sum_{ij}P_{ij}=1$), we have

$$P_{ii}=\tfrac{1}{3}-2P_{ij} \ . \tag{8}$$

It follows from (5) that

$$2\dot{P}_{ij}=P_{ij}(2-27P_{ij}) \ . \tag{9}$$

From the above equation, we can easily prove that the stationary solution (6) (*symmetrical fixed point*) is stable under the condition (7).

Next, we consider general cases where the initial condition never satisfies the relation (7). We solve the basic equations (5) by computer simulation. In Fig. 2, a typical example of time dependences of densities is displayed. The population dynamics of PA shows that the symmetrical fixed point (6) becomes unstable. In order to

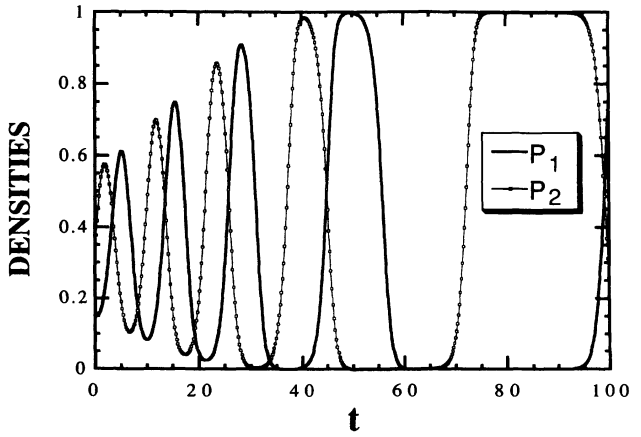

FIG. 2. A typical example of population dynamics under the pair approximation (PA). The time dependences of densities are displayed under the initial condition that $P_1=\frac{1}{6}$, $P_2=\frac{1}{3}$, $P_3=\frac{1}{2}$, and $P_{ij}=P_iP_j$.

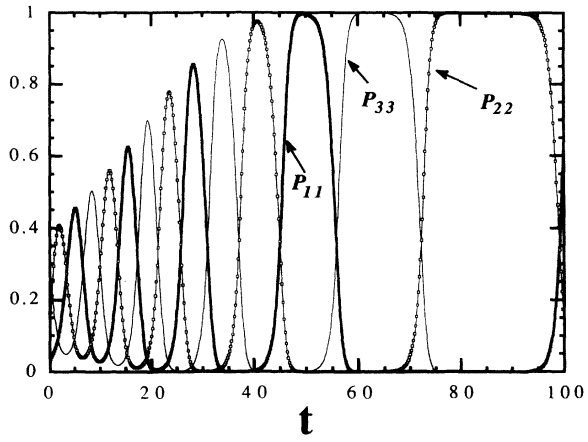

FIG. 3. The same as Fig. 2, but where the longitudinal axis denotes P_{ii} $(i=1,2,3)$.

give a detail of the attractor, we depict the time dependences of P_{ii} and P_{ij} in Figs. 3 and 4, respectively. It is found from Figs. 2–4 that the orbit in phase space is attracted into a cycle that contains the following three singular points (*asymmetrical fixed points*):

$$P_{11}=1, \quad P_{22}=1, \quad P_{33}=1 \ . \tag{10}$$

Although each point $P_{ii}=1$ is the stationary solution of (5), the orbit is never completely trapped into these states. When t is sufficiently large, the orbit stays in the vicinity of one of the asymmetrical fixed points for a very long period. It is therefore concluded that the symmetrical fixed point (6) is unstable, unless the special condition (7) is satisfied (saddle point).

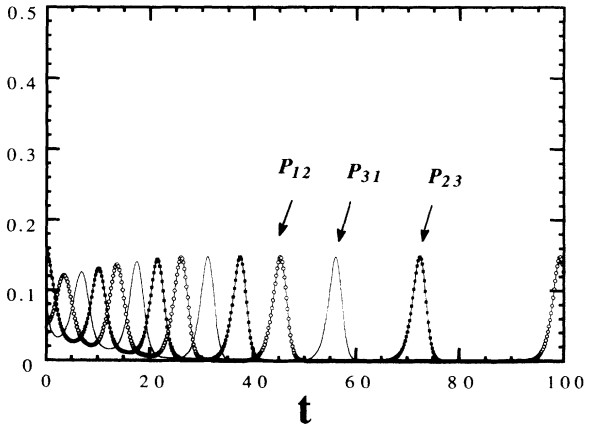

FIG. 4. The same as Fig. 2, but where the longitudinal axis denotes P_{ij} $(i\neq j)$.

IV. LONG-RANGE CORRELATION

The failure of the mean-field theory and PA model implies that the long-range correlation is essentially important for the pattern formation. According to the master equations (2) and (3), n-body probability densities are represented by $(n+1)$-body ones. Hence, higher-order probability densities (long-range correlations) play an important role for the population dynamics.

In the stationary pattern shown in Fig. 1(b), we notice such a long-range correlation. For example, if one individual of a species is located in the sea (cluster) of another species, the former species is usually weaker than the latter one. This feature is related to higher-order probability densities, so that they are never explained by the usual correlation function.

We first define the usual correlation function C_{ij} as fol-

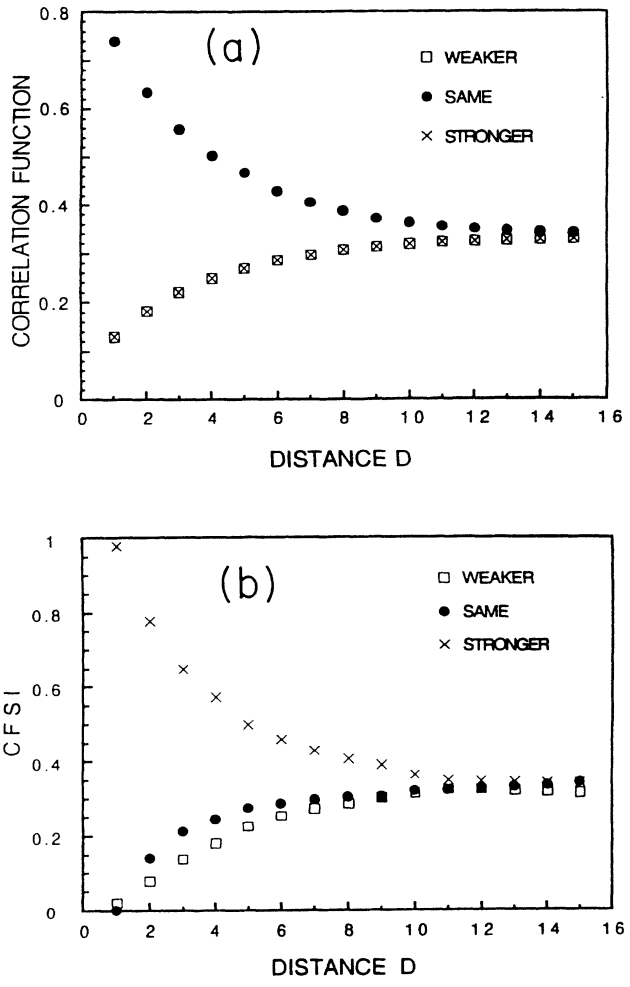

FIG. 5. Correlation functions obtained from the stationary pattern [Fig. 1(b)] are plotted against D, where (a) and (b) represent the usual correlation function (C_{ij}) and CFSI, respectively. The terms "weak," "same," and "strong" in this figure mean that the species i is weaker than, is of equal strength, and is stronger than the reference species j, respectively. The horizontal axis denotes the distance D, which is defined by the least number of lattice steps between two lattice points.

lows: C_{ij} is the probability of finding a species i under the condition that there is a reference individual of a species j at a distance D from species i. In Fig. 5(a), the correlation functions (C_{ij}) obtained from the stationary pattern [Fig. 1(b)] are plotted against D, where the terms "weak," "same," and "strong" in this figure mean that the species i is weaker than, of equal strength as, and stronger than the reference species j. We find from Fig. 5(a) that each species forms a contagious pattern ($C_{ii} > C_{ij}$, for $i \neq j$). However, the difference between weaker and stronger species is not shown in this figure.

Next, we define a correlation function for a surrounded individual (CFSI); CFSI is the correlation function under the condition that the reference individual is completely surrounded by another species. By definition, CFSI at $D=1$ for the same species takes the value of zero. In Fig. 5(b), the results of CFSI are displayed. It is found from Fig. 5(b) that the surrounded species is usually weaker than the surrounding one. Hence, the stationary pattern indicates the strength relation between species. Such an effect of long-range correlation is never taken into account in the pair approximation (4).

We show another example of long-range correlation. Although the configuration of the pattern in the quasistationary state dynamically varies, we can observe the following unchanged features.

(i) There are various sizes of clusters occupied by the same species (fractal-like pattern). In particular, several large clusters are observed [Fig. 1(b)].

(ii) We have shown power-law spectra in a limited frequency region [26].

The above results (i) and (ii) may be related to each other, i.e., the low-frequency components in the power-law spectra are associated with the fact that it takes a long time for a large cluster to change its shape. This will be qualitatively discussed in the next section.

V. DEFECT DYNAMICS

The pattern dynamics of the PFR is never explained by the mean-field theory nor by pair approximation. In general, it is very difficult to give a theoretical approach on the dynamics of spatial patterns. This difficulty mainly lies in the fact that the number of total lattice sites is very large. Now we introduce the concept of topological defects [2] to understand the pattern dynamics. The importance of topological defects is widely recognized in many areas. Since the number of topological defects is much less than that of total lattice sites, the pattern process of the system is very simplified.

A. Vortex

We first consider the pattern formation in two-dimensional lattice space. We define "domain (cluster)" as the region occupied by individuals (particles) of the same species. Even in the stationary state, the configuration of domains greatly varies with time. Let us define "average velocity" with respect to the movement of the domain boundary: when the species at neighboring lattice points are i and j ($i \neq j$), the average velocity v_{ij} of the boundary takes a constant vector (v, $-v$, or 0):

$$\begin{aligned} &v_{12}=v_{23}=v_{31}=v \ , \\ &v_{21}=v_{32}=v_{13}=-v \ , \\ &v_{ii}=0 \ . \end{aligned} \tag{11}$$

We consider a unit square cell that contains four particles. In each cell, four velocity vectors can be determined. From these vectors, we define the "vorticity" ω at the center of the cell by

$$\omega = \mathrm{curl} v, \tag{12}$$

which is calculated from (11) in a difference scheme of rotation:

$$\omega = 3v\nu n \ , \quad \nu = 0, 1, -1 \ . \tag{13}$$

Here n is the unit vector normal to the lattice plane, and ν is the vortex charge. The above equation shows that there are two types of vortices, V_R ($\nu=1$) and V_L ($\nu=-1$), distinguished by the vortex charge (direction of the rotation). From the Stokes theorem in the discrete version, we find the conservation law, that is, that the total vortex charge always vanishes under the periodical boundary condition. This law explains the following vortex reaction:

$$V_R + V_L \rightleftharpoons \phi \ . \tag{14}$$

Although the vortex moves in a complicated manner as a particle, it is never annihilated nor created except for the reaction (14).

B. Dynamics of the vortex

We performed the simulation of the position-fixed reaction and obtained the time dependences of the total number (density) of vortices $N(t)$ for different initial conditions (Fig. 6). It is found from Fig. 6 that $N(t)$ reaches

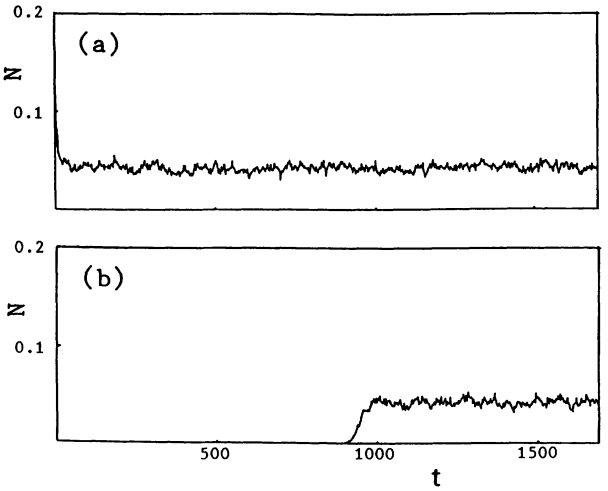

FIG. 6. The time dependences of the total number (density) of vortices $N(t)$. Initial conditions are chosen as follows: (a) random pattern; (b) three species distribute as a tricolor flag.

a stationary value, irrespective of the initial conditions. Moreover, we find from Fig. 6(b) that it takes a long time to reach the stationary state for the initial condition $N(0)=0$. Snapshots of the vortex pattern are displayed in Fig. 7, where (a) and (b) represent the initial and stationary states, respectively. Although the defect pattern in the stationary state greatly varies with time, it has invariant features. First, there are large voids where the vortex is empty. Second, vortices are located with negative correlation; the type V_R is located around a vortex of type V_L.

In Fig. 8, the number of vortices that are created or annihilated during one MCS are plotted, where the initial pattern is set as the random distribution. For the sake of comparison, $N(t)$ is also shown in this figure. From Fig. 8, we obtain the dependences of creation and annihilation rates against N (Fig. 9). It is found from Fig. 9(a) that the creation rate is proportional to the total vortex number N. On the other hand, Fig. 9(b) reveals that the annihilation rate of vortices is proportional to N^2. This result implies that the annihilation process takes place by a random collision of a vortex pair. In summary, we obtain the dynamical equation for the density of vortices N:

$$\dot{N}=\alpha N-\beta N^2 , \tag{15}$$

where $\alpha=0.59$ and $\beta=6.9$ (density^{-1}). The above equation represents the fact that the density of the vortices reaches a stationary value: $N_S=\alpha/\beta\sim 0.09$. Thus the defect dynamics explain well the stabilization of pattern dynamics. It is, however, noted that the stationary value N_S is considered different from the result obtained by actual simulation. In the latter case, we have $N_S\sim 0.04$.

We can visualize the defect dynamics by the use of a video. Observation of defect dynamics shows the following results.

(a) The vortices are not equally created at every site ("unequal creation"). The creation rate decreases in a region where the density of the vortex is low.

(b) The migration of the vortex is not random ("non-random walk"). It is very rare that a vortex moves into a large void. The vortex has a tendency to go to the region where vortices are rich.

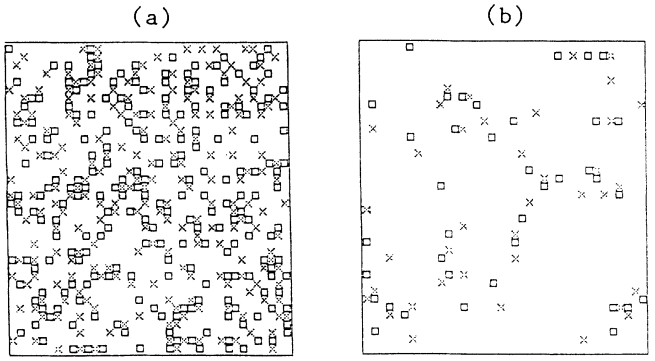

FIG. 7. Typical pattern formation of vortices in two-dimensional square lattice space (38×38). (a) The vortex pattern at $t=0$, where species distribute randomly. (b) A stationary pattern ($t=200$).

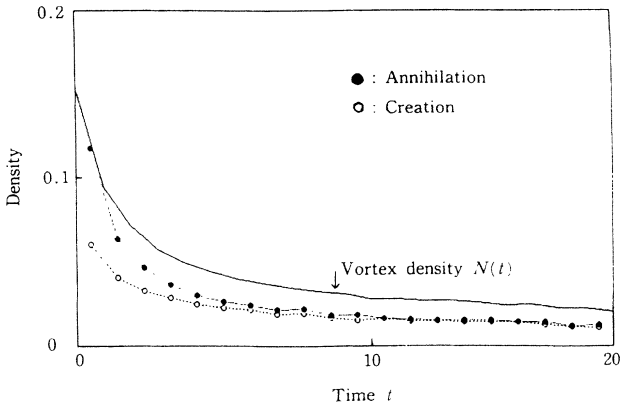

FIG. 8. The time dependence of the number (density) of vortices that are created or annihilated during one MCS. The total number of vortices N is also plotted in this figure. The initial pattern is set as the random distribution [Fig. 7(a)].

The results (a) and (b) can be easily understood by the following consideration. Inside a large void, a homogeneous pattern occupied by one species is usually formed, so that a vortex pair is hardly created in the void, or a vortex rarely goes into the void.

Finally, we emphasize the following points.

(i) If a fluctuation term is added to the right hand side of (15), then we may obtain similar defect dynamics as

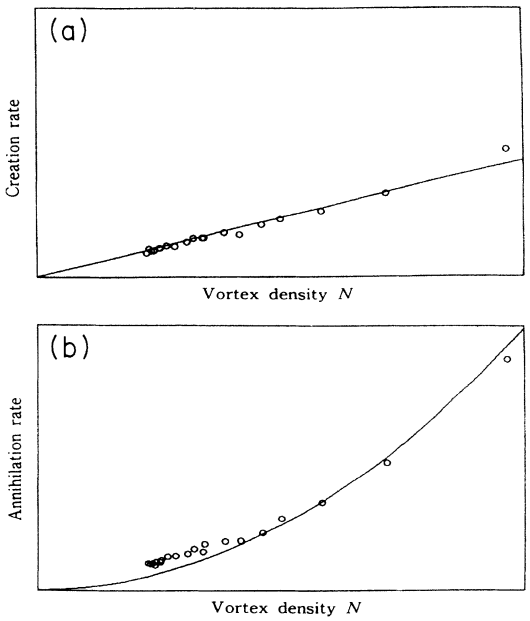

FIG. 9. The dependences of creation and annihilation rates against N. These figures are obtained from the results of Fig. 8; (a) creation rate, (b) annihilation rate. The line in (a) represents αN, while the curve in (b) denotes βN^2, where $\alpha=0.59$ and $\beta=6.9$ (density^{-1}).

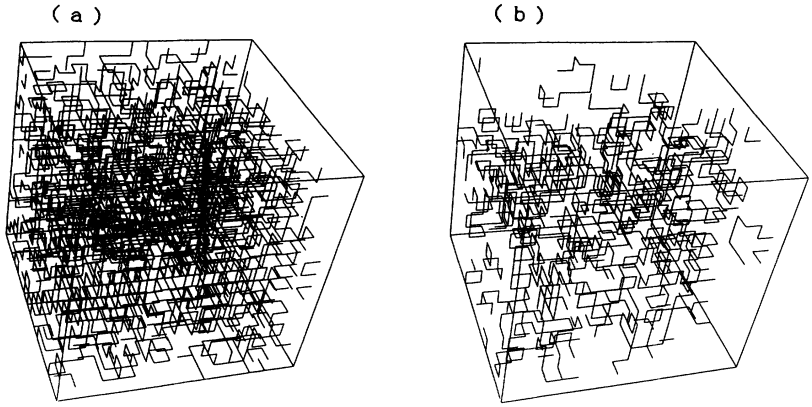

FIG. 10. Typical pattern formation of strings in three-dimensional cubic lattice space ($16\times16\times16$). (a) The string pattern at $t=0$, where species distribute randomly. (b) A stationary pattern ($t=100$).

shown in Figs. 6(a) and 6(b).

(ii) The unequal creation and nonrandom walk of the vortex qualitatively account for the fact that the local density of the vortex largely differs from the overall (average) density.

For reason (ii), a variety of sizes of clusters (fractal-like pattern) or large vortex voids are produced [see Fig. 1(b) or Fig. 7(b)]. Such large voids are related to the power-law spectra as described in the preceding section.

C. String

We describe the topological defects in the case where the spatial dimension d is high. If $d=3$, the defect is characterized by the vortex line (string), which is a sequence of vortices. Every string closes, under the periodical boundary condition. Since the species rotate around the string (loop), each string has its own direction of rotation.

We performed the simulation of the position-fixed reaction (PFR) and obtained the time dependences of the string pattern. An example of pattern formation is illustrated in Fig. 10, where (a) and (b) represent the string patterns at the initial and stationary states, respectively. The string dynamics for the PFR system reveals that the total length of the strings (L) approaches a unique value (stationary state); $L\sim0.12$. In this process, each string grows or shrinks and sometimes gives rise to reconnection. Thus, our strings resemble the vortex lines in superfluid [27] or the comic strings [28]. However, the string in our model has several properties that are different from other strings: (i) strings can be created inside the system; (ii) our string is discrete. By the latter feature, we can easily find the elementary process of the string dynamics,

$$U_R \rightleftharpoons \phi \ , \tag{16}$$

where U_R is the smallest unit ring. For the cubic lattice, U_R denotes the square loop with a side of the lattice size. There are two types of loops, which are distinguished by the directions of rotation. Whenever the strings change their shape, the unit ring U_R of the defect is annihilated or created for one collision step.

The process leading to the stationary state is very complicated, depending on initial conditions. Another example of pattern formation is illustrated in Fig. 11, where (a) represents the distribution of species at $t=0$ (the string is therefore absent). The configurations of strings are visible in Figs. 11(b), 11(c), and 11(d). In the early-time stage ($t=\frac{1}{4}$) several unit rings are created. The axes of the rings point in the same direction, since the creation of the rings is attributed to the fact that species 3 in Fig. 11(a) connects with 1 penetrating 2. The snapshots in the steady state [Figs. 10(b) and 11(d)] illustrate several features: (i) large voids are found as for $d=2$; (ii) the shape of the large strings is entangled in a complicated way. These features are also explained by the unequal

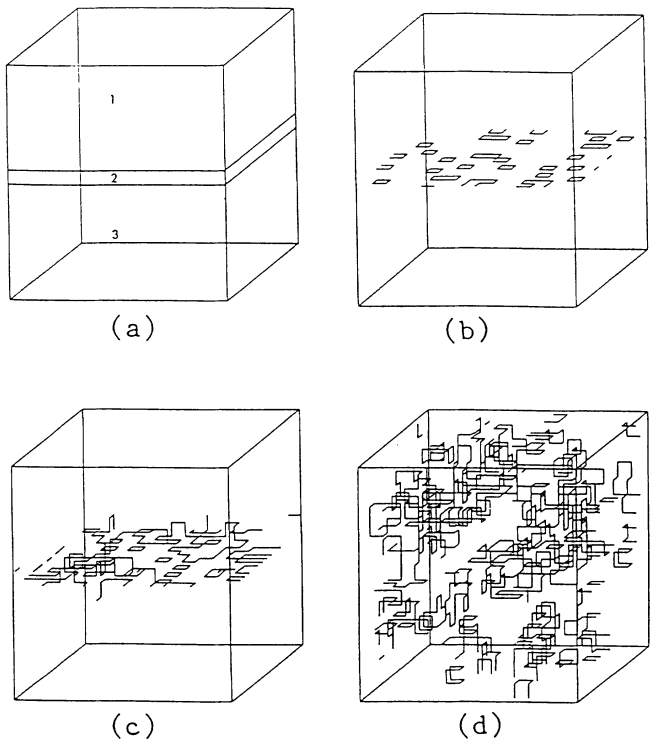

FIG. 11. The same as Fig. 10, but an initial pattern of three species is distributed as shown in (a). String configurations are displayed in (b) and (c), where (b) $t=\frac{1}{4}$, (c) $t=1$, and (d) $t=100$ (stationary state).

creation of vortex rings. In the region where string density is high, many unit rings are frequently created or annihilated. Under such a situation, the string forms a complicated configuration.

VI. CONCLUSIONS AND DISCUSSION

We have studied the dynamics of the PSS model. It is well known that the position-fixed reaction (PFR) of this model is self-organized into a stationary state irrespective of initial patterns. The mean-field theory (MFT) never predicts such a dynamics. In the present article, we examined the population dynamics in the pair approximation limit, which corresponds to the second order approximation for the lattice model (PFR). Numerical analysis reveals that in the PA limit the symmetrical fixed point ($P_1=P_2=P_3=\frac{1}{3}$) becomes unstable (saddle point). It is therefore found that the PA never sufficiently explains the result of the lattice model, compared to the MFT. We schematically illustrate the results of the dynamics in three different methods:

Symmetrical fixed point ———
- PFR ———stable focus
- MFT ———neutrally stable center
- PA ———unstable saddle point .

In the case of the PA model, the orbit in phase space is attracted to the cycle that contains the asymmetrical fixed points (10). The failure of the mean-field theory and PA model may come from the fact that these theories neglect the effect of long-range correlation [11].

In Sec. IV, we have described the effect of long-range correlation. The stationary pattern in PFR [Fig. 1(b)] is formed under such an effect. For example:

(i) If one individual of a species is located in the cluster (domain) of another species, the former species is usually weaker than the latter one.

(ii) There are various sizes of clusters occupied by the same species (fractal-like pattern).

Feature (ii) is qualitatively explained by the concept of a vortex, the formation of the fractal-like pattern may originate in the properties of unequal creation and the nonrandom walk of the vortex as described in Sec. V. As for feature (i), its mechanism is still unknown, and a more refined theory or idea will be necessary.

We have demonstrated the dynamics of topological defects. Since the number of topological defects is much less than that of total lattice sites, the pattern formation in the lattice system is simplified by defect reactions. The creation (or annihilation) rate of vortices is proportional to N (or N^2). It is therefore found that the creation process is similar to the photon creation in stimulated emission, while the annihilation process closely resembles usual random collision between vortex pairs. Such a difference between creation and annihilation processes accounts well for the stabilization of population dynamics [see (15)]. It is therefore important to take into account the effect of long-range correlation (mesoscopic effect).

We discuss the topological defects when the spatial dimension d is high. In the string system ($d=3$), we presented (16) as the elementary process of the dynamics. Thus the defect dynamics explains well the stabilization of pattern dynamics in $d=3$. It is natural to conclude from (16) that for the order parameter, using the number of unit rings U_R to construct a whole string is more appropriate than using the total length of strings (L). Unfortunately, however, it is difficult to obtain this value from the actual lattice system.

If $4 \leq d$, the topological defect is known as a "membrane." From the analogy with (16), we easily predict that the elementary process of defect dynamics is represented as follows:

$$U_S \rightleftharpoons \phi \ , \tag{17}$$

where U_S is the $(d-2)$-dimensional unit surface. In the case of a four-dimensional lattice, U_S denotes the surface of the unit cubic with a side of the lattice size. There are two types of unit surfaces which are distinguished from the directions of rotation. Whenever the membrane changes its shape, the unit surface U_S of the defect may be annihilated or created for each collision step.

ACKNOWLEDGMENT

The author wishes to express his thanks to Professor Y. Itoh for many valuable discussions.

[1] G. Nicolis and I. Prigogine, *Self-organization in Nonequilibrium Systems* (Wiley, New York, 1977); H. Haken, *Synergetics—An Introduction* (Springer-Verlag, Berlin, 1978); Los Alamos Center for Nonlinear Studies Workshop on Spatio-temporal Coherence and Chaos in Physical Systems [Physica D **23** (1986)]; P. Manneville, *Dissipative Structures and Weak Turbulence* (Academic, New York, 1990); E. A. Jackson, *Perspectives of Nonlinear Dynamics* (Cambridge University Press, Cambridge, 1991), Vol. 2.

[2] K. Tainaka, Phys. Rev. Lett. **63**, 2688 (1989).
[3] R. Balian, M. Kelman, and J. P. Poirier, *Physics of Defects* (North-Holland, Amsterdam, 1981).
[4] K. Tomita and H. Tomita, Prog. Theor. Phys. **74**, 1731 (1974); K. Tainaka, S. Kanno, and T. Hara, *ibid.* **80**, 199 (1988).
[5] Y. Itoh, Proc. Jpn. Acad. **47**, 854 (1971); **51**, 374 (1975); J. Appl. Prob. **16**, 36 (1979); Prog. Theor. Phys. **78**, 507 (1987); J. Phys. Soc. Jpn. **62**, 1826 (1993).
[6] K. Tainaka, J. Phys. Soc. Jpn. **57**, 2588 (1988); K. Tainaka and Y. Itoh, Europhys. Lett. **15**, 399 (1991).
[7] M. Bramson and D. Griffeath, Ann. Prob. **17**, 26 (1989).
[8] S. A Levin, *Lectures in Mathematics* (Kinokuniya, Tokyo, 1976), Vol. 8, pp. 1–35; L. L. Cavalli-Sforza and M. W. Feldman, *Cultural Transmission and Evolution* (Princeton University Press, Princeton, 1981); G. Ertl, Science **254**, 1750 (1993).
[9] J. Hofbauer and K. Sigmund, *The Theory of Evolution and Dynamical Systems* (Cambridge University Press, Cambridge, 1988); N. S. Goel, S. C. Maitra, and E. W. Montroll, Rev. Mod. Phys. **43**, 231 (1971).
[10] K. Tainaka, J. Theor. Biol. **164**, 91 (1994).
[11] K. Sato, H. Matsuda, and A. Sasaki, J. Math. Biol. **32**, 251 (1994).
[12] S. Wolfram, Rev. Mod. Phys. **55**, 601 (1983).
[13] J. P. Crutchfield and K. Kaneko, *Directions in Chaos* (World Scientific, Singapore, 1987); K. Kaneko, Physica D **41**, 137 (1990).
[14] D. Toussaint and F. Wilczeck, J. Chem. Phys. **78**, 2642 (1983); K. Kang and S. Redner, Phys. Rev. A **32**, 435 (1985); G. Zumofen, A. Blumen, and J. Klafter, J. Chem. Phys. **82**, 3198 (1985); S. Kanno, Prog. Theor. Phys. **79**, 1330 (1988); S. Kanno and K. Tainaka, J. Phys. Soc. Jpn. **62**, 2275 (1993).
[15] L. W. Anacker and T. Kopelman, Phys. Rev. Lett. **58**, 289 (1987); S. Kanno and K. Tainaka, Prog. Theor. Phys. **80**, 999 (1988).
[16] K. Tainaka and S. Fukazawa, J. Phys. Soc. Jpn. **61**, 1891 (1992); K. Tainaka, *ibid.* **61**, 4257 (1992); K. Tainaka, S. Fukazawa, and S. Mineshige, Publ. Astron. Soc. Jpn. **45**, (1993), pp. 57–64 and Plate 1.
[17] K. Tainaka, Phys. Lett. A **176**, 303 (1993).
[18] K. Tainaka and Y. Itoh, Phys. Lett. A **187**, 49 (1994).
[19] F. Schlogl, Z. Phys. **253**, 147 (1972); R. C. Brower, M. A. Furman, and M. Moshe, Phys. Lett. B **76**, 213 (1978).
[20] R. Durrett, *Lecture Notes on Particle Systems and Percolation* (Wadsworth & Brooka/Cole Advanced Books & Software, Belmont, CA, 1988).
[21] M. Katori and N. Konna, J. Stat. Phys. **63**, 115 (1991).
[22] K. Tainaka, Chaos, Solitons, Fractals (to be published).
[23] R. T. Paine, Oecologia **15**, 93 (1974); P. Yodgis, Ecology **69**, 508 (1988); J. Vandermeer, J. Theor. Biol. **148**, 545 (1991).
[24] M. Katori and N. Konno, J. Phys. Soc. Jpn. **60**, 418 (1991); N. Konno and M. Katori, *ibid.* **59**, 1581 (1990); **61**, 806 (1992).
[25] H. Matsuda *et al.*, Prog. Theor. Phys. **88**, 1035 (1992).
[26] Y. Itoh and K. Tainaka, Phys. Lett. A **189**, 37 (1994).
[27] K. W. Schwarz, Phys. Rev. Lett. **49**, 283 (1982).
[28] D. P. Bennett and F. R. Bouchet, Phys. Rev. Lett. **60**, 257 (1988); A. Albrecht and N. Turok, Phys. Rev. D **40**, 973 (1989).

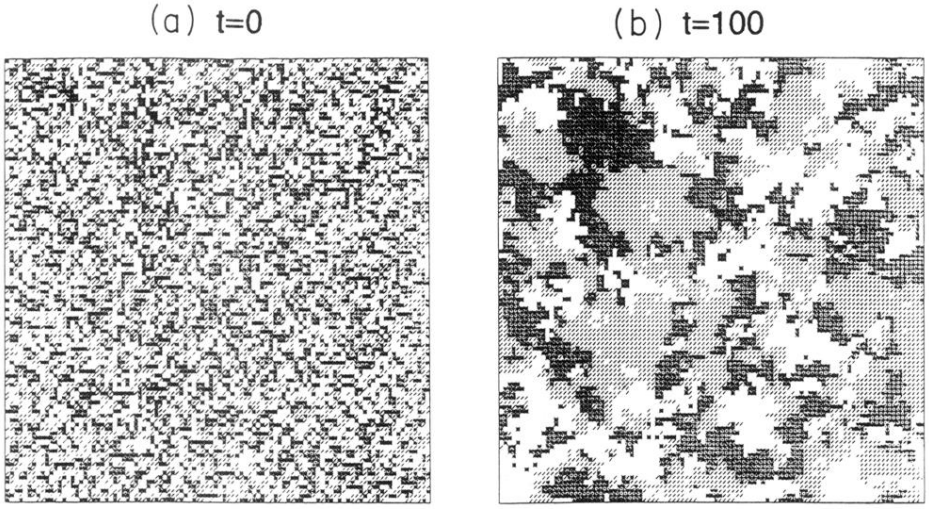

FIG. 1. Photographs of typical patterns are illustrated, where (a) and (b) represent the initial random pattern and final stationary pattern, respectively.